

BAND GAP OF CUBIC AND HEXAGONAL CDS QUANTUM DOTS - EXPERIMENTAL AND THEORETICAL STUDIES

NAYEREH SOLTANI*, ELHAM GHARIBSHAHI, ELIAS SAION

*Department of Physics, Universiti Putra Malaysia, 43400 UPM Serdang,
Selangor, Malaysia*

CdS quantum dots of face centered cubic (fcc) and hexagonal close packed (hcp) structures were synthesized from sulphur source of sodium sulphide and thioacetamide respectively via microwave-hydrothermal method. The synthesized quantum dots were characterized using X-ray diffraction (XRD), transmission electron microscopy (TEM) and UV-visible spectrophotometry. The average particle size in the range 8.5 - 12.5 nm increases with the increase of microwave exposure time from 10 to 40 min. Particles with hcp structure are larger than those with the fcc structure. The band gap in the range 2.54 - 2.65 eV decreases with the increase of microwave exposure time and the particles with the hcp structure have larger band gap than those with the fcc structure. The band gap of the CdS quantum dots were also derived from time independent Schrodinger equations for CdS system and calculated using the density functional theory (DFT). There is good agreement between the measured and calculated band gap values. The results also reveal that the band gap decreases with the increase of particle size due to the quantum size effects.

(Received July 9, 2012; Accepted July 30, 2012)

Keywords: CdS quantum dots, Optical absorption, Band gap, DFT, Crystal structures, Particle size

1. Introduction

II-IV binary compound semiconductors, including cadmium sulfide (CdS) quantum dots (QDs) have traditionally shown remarkable fundamental optical and electrical properties. CdS is a well-known direct band gap semiconductor having both zincblende and wurtzite crystal structures. In recent years, the progress of new synthesis methods intended for demonstrating quantum size effects of nanoscale CdS has attracted considerable attention because of unique optoelectronic, photochemical, and photocatalytic properties that are dramatically different from their bulk counterparts [1]. CdS quantum dots exhibit unique size-tunable optical and electronic properties such as band gap widening, change of electrochemical potential of band edge, and enhancement of photocatalytic activities with decreasing crystallite size [2-10]. These properties are due to a large number of surface atoms and three-dimensional confinement electrons [11-12]. Hence, the study of the quantum confinement in this semiconductor has been a subject of intense research. The increase of the band gap upon a decrease of particle size is one of the characteristics which can be observed by optical absorption spectroscopy. Upon a decrease of the particle radius, the onset of the absorption shifts towards higher energy.

To compute a band gap of quantum dots theoretically, it is easier to calculate of optical absorption energy of electronic transitions between the valence and conduction bands of quantum dots. The transitions happen when incident photons strike the quantum dots and the valence band electrons of Cd atoms absorbed photons and excited to higher energy level of the conduction band of S atoms. Since, the band gap energy of quantum dots is dependent on particle size and lattice

*Corresponding author: nayereh.soltani@gmail.com

structure, to understand the transitions between the electronic states requires a quantum theory treatment. An approach based on the density functional theory (DFT) should enable physicists to simulate the electronic transitions for determining the band gap of quantum dots. Several theoretical approaches have been proposed to compute electronic structure of quantum dots and most of them are identical to the ones used to study atoms and molecules. Quantum dots based on atomic structure have three-dimensional electronic confinement of the energy level degeneracy, orbital structure and spin correlation [13-17].

In view of the fact that breakthrough in nanoscience is becoming progressively dependent on simulation and modeling, the present article is dedicated to the measurement and computation of optical band gaps of different size CdS quantum dots having the lattice structure of face centered cubic (fcc) and hexagonal close packed (hcp). Microwave irradiation method was used to synthesis CdS nanoparticles with different size and different crystal structures. The size of CdS nanoparticles was dictated by changing in microwave irradiation time from 10 to 40 min and the control over crystal structure of nanoparticles was performed by changing in sulfur source. Sodium sulphide (Na_2S) and thioacetamide ($\text{C}_2\text{H}_5\text{NS}$) were used as sulfur sources to obtain cubic and hexagonal structure CdS nanoparticles, respectively [18]. The experimental band gaps are therefore compared with the theoretical band gaps.

2. Materials and methods

2.1 Experimental

The starting materials for the synthesis of CdS nanoparticles were cadmium chloride (Acros Organics) as cadmium source, sodium sulphide (R & M Chemical) and thioacetamide (Sigma-Aldrich) as sulfur sources and distilled water as solvent. All chemicals were analytical grade products and used without further purification.

In a typical synthesis, 0.005 M of cadmium chloride and 0.006 M of sulfur source (sodium sulphide for fcc structure or thioacetamide for hcp structure) were added into 100-ml glass beakers containing 20 ml of distilled water and stirred with 500 rpm for 30 min. The beakers were placed in a high power microwave oven (1100 W) operated using a pulse regime with 20% power for different irradiation time from 10 to 40 min. The precipitates were centrifuged (3500 rpm, 10 min) and washed several times with distilled water and absolute ethanol. The yellow products were dried in air at 60°C for 24 h under control environment. The products were characterized by X-ray diffraction (XRD) at a scanning rate of 5°/min in the 2θ range 20–70° using a Philips X-ray diffractometer (7602 EA Almelo) with Cu Kα radiation ($\lambda = 0.1542$ nm). The particle size and size distribution were determined from the transmission electron microscopy (TEM) micrographs (HTACHI H-7100 TEM). The TEM characterization was carried out at 100 keV. The optical properties of ZnS nanoparticles were characterized using UV–visible absorption spectroscopy (UV-1650PC SHIMADZU).

2.2 Theoretical

The band gaps of the CdS quantum dots of different crystal structures were calculated according to our previous work [19]. The quantum dots were considered an isolated spherical nanoparticle containing N atoms confined in a face-centered cubic structure or in a hexagonal lattice structure. When light strikes CdS nanoparticle, electrons at the valence band state of Cd absorbed photon energy and excited to the conduction band state of S. The total functional energy may take in the form:

$$E[\rho] = C_K \int \rho(r)^{5/3} dr + \frac{\eta}{8} \int \frac{|\nabla \rho(r)|^2}{\rho(r)} dr + \int \rho(r) v(r) dr + \frac{1}{2} \iint \frac{\rho(r)\rho(r')}{|r-r'|} dr dr' - C_e \int \rho(r)^{4/3} dr \quad (1)$$

The Euler equation (1) may be presented in terms of functional derivatives:

$$\frac{5}{3} C_k \int \rho(r)^{2/3} dr + \frac{\eta}{8} \left[\frac{|\nabla \rho(r)|^2}{\rho(r)^2} - 2 \frac{\nabla^2 \rho(r)}{\rho(r)} \right] + v(r) + e^2 \int \frac{\rho(r)}{|r-r'|} dr - \frac{4}{3} C_e \int \rho(r)^{1/3} dr = \mu \quad (2)$$

where r is the displacement coordinate of the electrons from the centre of a sphere and is dependent on the quantum numbers n , l , and s . For a completely degenerate electron gas at absolute zero temperature, μ is the Fermi energy, and $v(r) = v_1(r_1) + v_2(r_2)$ is the summation of nuclear potentials of each atomic element of the QDs. We found that the density of conduction electrons $\rho(r)$ of an atom is a function of atomic number Z and absorption $\sigma(r)$. Since both $\rho(r)$ and $\sigma(r)$ are continuous functions, the transformation of the density functional energy E to the absorption functional energy $E[\rho]$ can be made by algebraically substituting the electron density function with the absorption function in the Euler-Lagrangian equation (2). The absorption function $\sigma(r)$ was derived in terms of the electronic density $\rho(r)$. Taking the wavelength of electrons in the valence band to conduction band transition as λ and the absorption $\sigma(r)$, the total energy functional Euler-Lagrange equation can then be written in terms of $\sigma(\lambda)$ as a function of λ with the boundary conditions $\sigma_0 = 0$ and $\sigma_N = 0$. For a numerical calculation, λ and $\sigma(\lambda)$ may be discretized into σ_i and λ_i , where $i = 0, 1, 2, \dots, N$, and N is the number of atoms that made up the QD size. The final Euler-Lagrange equation can be expressed in finite differences, and the multivariable equation can be solved. For QDs, the highly occupied state orbital electrons in the valence band absorb photons and transit to the higher energies of unoccupied state orbital in the conduction band. Hence, the coordinate r of the electron is dependent on the principle quantum number n , angular quantum number l , and spin quantum number s .

3. Results and discussion

The formation of CdS nanoparticles can be observed by changing in color of solution from colorless to yellow and confirmed by powder X-ray diffraction studies. Fig. 1 shows the XRD patterns of CdS nanoparticles synthesized with sodium sulphide and thioacetamide as sulfur sources. In this figure the peaks observed in the XRD patterns of CdS nanoparticles synthesized in sodium sulphide at 2θ values of 26.4, 43.8, 51.9 and 71.2, matched perfectly with the (111), (220), (311) and (331) crystalline planes of the face centered cubic structure of CdS (ICDD PDF 89-0440) with the crystal lattice parameter of 5.8 Å and the cell volume of 198.2 Å³. For CdS nanoparticles synthesized with thioacetamide, the peaks observed in the XRD patterns at 2θ values of 24.8, 26.5, 28.2, 36.6, 43.7, 47.8, 51.8, 67.1 and 75.9 matching perfectly with the (100), (002), (101), (102), (110), (103), (112), (203) and (204) crystalline planes of the hexagonal structure of CdS (ICDD PDF 77-2306) with the crystal lattice parameters of 4.1, 4.1 and 6.7 Å and the cell volume of 99.4 Å³.

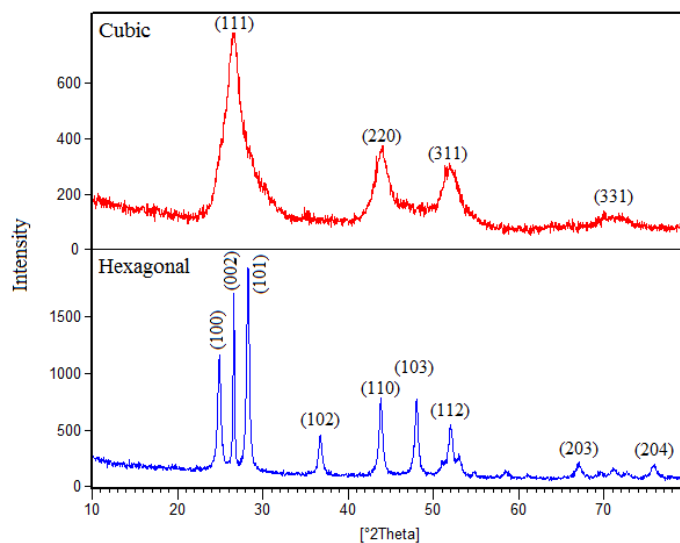


Fig. 1. XRD pattern of the CdS nanoparticles synthesized with (a) sodium sulphide for cubic structure and (b) thioacetamide for hexagonal structure.

Fig. 2 and Fig. 3 show the TEM images and corresponding size distribution histograms of CdS nanoparticles synthesized in 20 min irradiation time with sodium sulphide and thioacetamide, respectively. The figures indicate that CdS nanoparticles prepared with sodium sulphide are spherical in shape with sizes from 7 to 15 nm that are agglomerated. CdS nanoparticles synthesized with thioacetamide, on the other hand, are approximately monodispersed and have slightly larger sizes, estimated to be 8 to 16 nm.

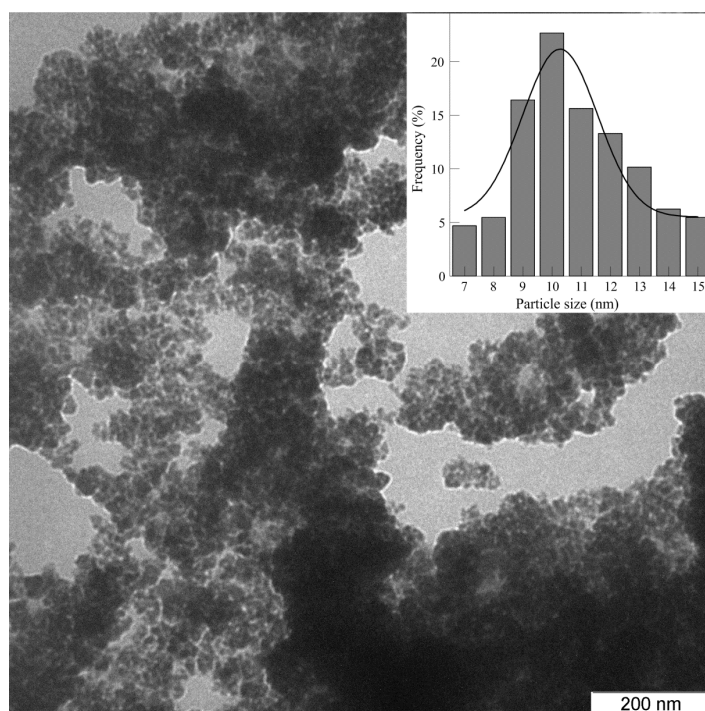


Fig. 2. TEM images and particle size distribution of CdS nanoparticles synthesized using sodium sulphide as sulfur source at 20 min irradiation time.

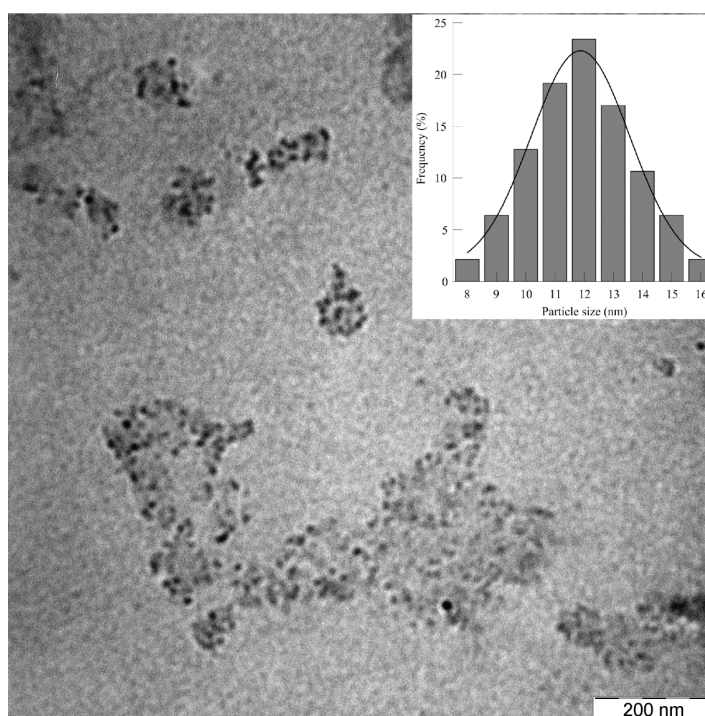


Fig. 3. TEM images and particle size distribution of CdS nanoparticles synthesized using thioacetamide as sulfur source at 20 min irradiation time.

Fig. 4 and Fig. 5 show the UV-Vis absorption spectra of CdS nanoparticles prepared in different irradiation times using sodium sulphide and thioacetamide as sulfur sources, respectively. The samples show a blue shift of the absorption edge compared to bulk CdS which is clearly explained by the quantum confinement effect.

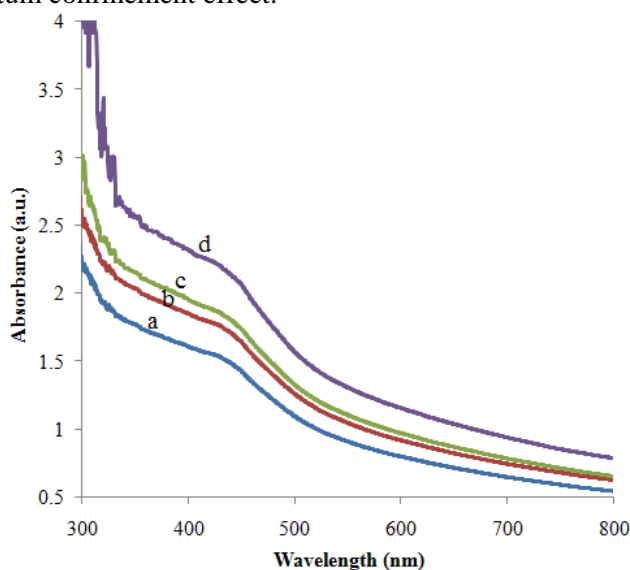


Fig. 4. UV-Visible spectra of CdS nanoparticles synthesized using sodium sulphide as sulfur source at (a) 10, (b) 20, (c) 30 and (d) 40 min irradiation time.

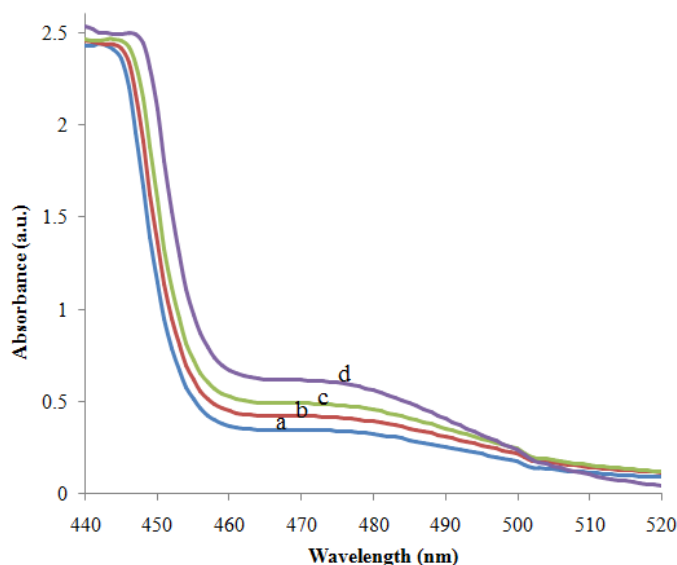


Fig. 5. UV-Visible spectra of CdS nanoparticles synthesized using thioacetamide as sulfur source at (a) 15, (b) 20, (c) 25 and (d) 40 min irradiation time.

The optical band gap of CdS nanoparticles can be determined from the absorption spectra. In Tauc region (high absorption region) the absorption is due to interband transition among extended states in both valence and conduction bands and the absorption coefficient depends on optical band gap, given by:

$$\alpha(\nu) = K(h\nu - E_g)^n/h\nu \quad (3)$$

where E_g represents the optical band gap, K is a constant, and n depends on the nature of the transition which has values of 1/2, 3/2, 2, and 3 for allowed direct transitions, forbidden direct transitions, allowed indirect transitions, and forbidden indirect transitions, respectively [20-21]. The energy of band gap (E_g) can be evaluated from the UV-Vis spectra by plot of

$d(\ln(\alpha hv))/d(hv)$ versus (hv) which shows the discontinuity position assigned to the band gap value (at $hv - E_g = 0$) according to [22-23]:

$$d(\ln(\alpha hv))/d(hv) = n/(hv - E_g) \quad (4)$$

The $d(\ln(\alpha hv))/d(hv)$ versus (hv) plots of CdS nanoparticles prepared with sodium sulphide and thioacetamide are shown in Fig. 6 and Fig. 7, respectively. Although the figures show peak instead discontinuity position which is due to our instrument limitation range over to measure absorbance, but still the band gap energy can be evaluated from the peak position. The values of estimated energy band gaps are listed in Table. 1.

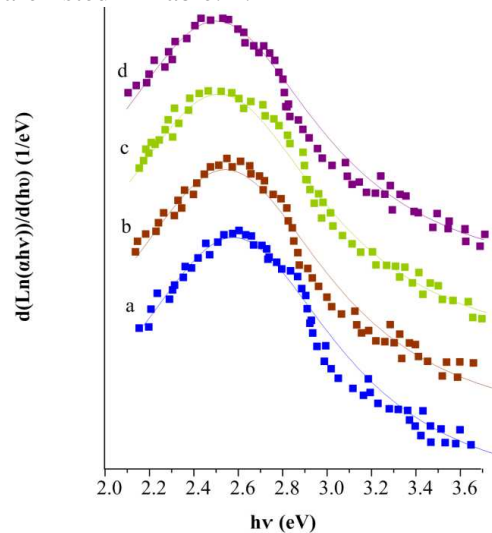


Fig. 6. $d(\ln(\alpha hv))/d(hv)$ vs. $h\nu$ plots for the CdS nanoparticles synthesized using sodium sulphide as sulfur source at different irradiation time.

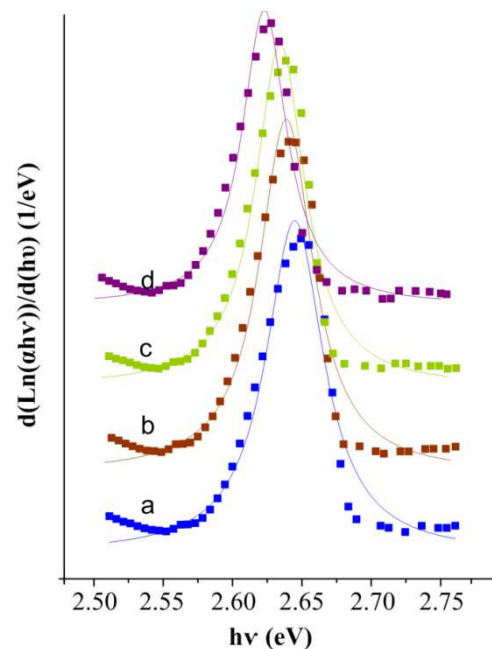


Fig. 7. $d(\ln(\alpha hv))/d(hv)$ vs. $h\nu$ plots for the CdS nanoparticles synthesized using thioacetamide as sulfur source at different irradiation time.

Table 1. Optical band gaps of CdS quantum dots estimated from the theory and experiment.

Sample No	Sulfur source	Structure	Irradiation time (min)	Particle size from TEM (nm)	Band gap from experiment (eV)	Band gap from theory (eV)
1	Na ₂ S	fcc	10	8.5	2.61	2.62
2	Na ₂ S	fcc	20	10	2.58	2.58
3	Na ₂ S	fcc	30	11	2.56	2.55
4	Na ₂ S	fcc	40	12	2.54	2.53
5	TAA*	hcp	15	10	2.65	2.62
6	TAA	hcp	20	11	2.64	2.60
7	TAA	hcp	25	11.5	2.63	2.58
8	TAA	hcp	40	12.5	2.62	2.57

*TAA: thioacetamide

The calculated absorption spectra were computed in terms of absorbance versus wavelength for both fcc and hcp CdS quantum dots at different particle sizes to determine the optical band gaps and as listed in Table 1. The absorption spectra display a red shift with increasing particle diameter due to the quantum size effects. For fcc structure, the absorption peaks of CdS QDs with particle size of 8.5, 10, 11, and 12 nm appear at the visible bands of 473, 480, 486, and 490 nm which correspond to the band gap of 2.62, 2.58, 2.55, and 2.53 eV respectively. For hcp structure, the absorption peaks of CdS QDs with particle size of 10, 11, 11.5 and 12.5 nm appear at the visible bands of 473, 476, 480 and 482 nm which correspond to the band gap of 2.62, 2.60, 2.58 and 2.57 eV, respectively.

4. Conclusions

CdS quantum dots with the particle size in the range 8.5–12.5 nm have been synthesized by microwave-hydrothermal method and resulted in face centered cubic and hexagonal close packed structures from using sodium sulphide and thioacetamide as sulphur source respectively. The band gap in the range 2.54–2.65 eV decreases with the increase of microwave exposure time and the particles with hexagonal structure have larger band gap than those particles with cubic structure. The calculated band gaps derived from time independent Schrodinger equations using the DFT method were found to agree fairly well with the experimental results. By increasing particle diameter from 8.5 to 12 nm for cubic structure of CdS quantum dots, a nonlinear red-shift of the energy band gap was observed from 2.62 to 2.53 eV in theory and from 2.61 to 2.54 eV in experimental results. Such red-shift of energy band gap was also detected for hexagonal structure of CdS quantum dots from 2.62 to 2.57 eV in theory and from 2.65 to 2.62 eV in experimental results when particle diameter increases from 10 to 12.5 nm.

Acknowledgment

This work was supported by the Ministry of Higher Education of Malaysia under the FRGS and RUGS grants. The authors would also like to thank staff of the Faculty of Science and the Bioscience Institute of University Putra Malaysia, who had contributed to this work.

References

- [1] L.S. Devi, K.N. Devi, B.I. Sharma, and H.N. Sarma, *Chalcogenide Letter*. **9**, 67 (2012).
- [2] S.H. Liu, et al., *J. Phys. Chem. Solids*. **64**, 455 (2003).
- [3] M. Pattabi, B. Saraswathi Amma, K. Manzoor, and S. Ganesh, *Sol. Energ. Mat. Sol. C*. **91**, 1403 (2007).
- [4] D. Philip, *Physica E*. **41**, 1727 (2009).

- [5] N. Tomczak, D. Janczewski, M. Han, and G.J. Vancso, *Prog. Polym. Sci.* **34**, 393 (2009).
- [6] H. Qian, L. Li, and J. Ren, *Mater. Res. Bull.* **40**, 1726 (2005).
- [7] V. Purcar, et al., *Mol. Cryst. Liq. Cryst.* **483**, 244 (2008).
- [8] R. He, et al., *Colloid. Surface. A.* **220**, 151 (2003).
- [9] Z. Sedaghat, N. Taghavinia, G. Rastegarzadeh, and M. Marandi, *Synth. React. Inorg. Met. Org. Chem.* **37**, 387 (2007).
- [10] M. Li and J.C. Li, *Mater. Lett.* **60**, 2526 (2006).
- [11] Y. Wu, L. Wang, M. Xiao, and X. Huang, *J. Non-Cryst. Solid.* **354**, 2993 (2008).
- [12] C. Xu, Z. Zhang, and Q. Ye, *Mater. Lett.* **58**, 1671 (2004).
- [13] M. Fricke, et al., *Europhys. Lett.* **36**, 197 (1996).
- [14] S. Tarucha, et al., *Phys. rev. lett.* **77**, 3613 (1996).
- [15] H. Drexler, et al., *Phys. rev. lett.* **73**, 2252 (1994).
- [16] J.Y. Marzin, et al., *Phys. rev. lett.* **73**, 716 (1994).
- [17] L. Fonseca, J. Jimenez, J. Leburton, and R.M. Martin, *Phys. Rev. B.* **57**, 4017 (1998).
- [18] N. Soltani, et al., *J. Inorg. Organomet. Polym.* (2011).
- [19] E. Gharibshahi and E. Saion, *Mater. Res. Innov.* **15**, 67 (2011).
- [20] X. Xu, et al., *Appl. Catal. B.* **102**, 147 (2011).
- [21] R.S. Singh, S. Bhushan, A.K. Singh, and S.R. Deo, *Dig. J. Nanomater. Bios.* **6**, 403 (2011).
- [22] S. Kar and S. Chaudhuri, 1-D zinc sulfide nanostructures: synthesis and characterization, in *Focus on nanomaterials research*, Nova Science Publisher, New York (2006).
- [23] S. Kar and S. Chaudhuri, *Chem. Phys. Lett.* **414**, 40 (2005).